Available online at www.sciencedirect.com

ScienceDirect

Dyes and Pigments 76 (2008) 656–662

DYES and PIGMENTS

www.elsevier.com/locate/dyepig

Comparison of hydrogen peroxide-based processes for treating dye-containing wastewater: Decolorization and destruction of Orange II azo dye in dilute solution

J.M. Peralta-Hernández [a], Yunny Meas-Vong [a], Francisco J. Rodríguez [a], Thomas W. Chapman [a], Manuel I. Maldonado [b], Luis A. Godínez [a,*]

[a] *Electrochemistry Department, Centro de Investigación y Desarrollo Tecnológico en Electroquímica, Parque Tecnológico Querétaro Sanfandila, Pedro Escobedo 76700, Querétaro, Mexico*

[b] *Plataforma Solar de Almería-CIEMAT, Crta. Senés s/n, Tabernas, Almería 04200, Spain*

Received 6 July 2006; accepted 17 January 2007
Available online 20 January 2007

Abstract

This work was performed to compare several Advanced Oxidation Processes in the treatment of wastewater containing an organic dye. In particular, aqueous solutions containing 50 ppm Orange II (OG-II) in 0.05 M Na_2SO_4 at pH 3 and at room temperature were subjected to three different hydrogen peroxide-based oxidation processes in a recycle-batch reactor: Direct Photolysis, the Electro-Fenton process, and a Photoelectro-Fenton process with two different iron(II) concentrations (0.2 mM and 0.5 mM). By producing $^{\bullet}OH$ radicals as an active oxidant, all of these processes remove the color from the solution in a short time, but the Photoelectro-Fenton with the lower iron level performed best. It not only decolorized the solution in less than 5 min, but it also destroyed 80% of TOC in 60 min of treatment. The comparable TOC removal efficiency was 63% for the Electro-Fenton system and only 31% for Direct Photolysis. It was found that higher levels of catalytic iron ions are detrimental to the Fenton-based processes.

Keywords: Electro-Fenton; Hydrogen peroxide; Orange II; Photoelectro-Fenton

1. Introduction

Dyeing and finishing operations produce large quantities of wastewater that contains organic dyestuff, surfactants, chelating agents, and other contaminants that can be characterized as high levels of total organic content and of color [1]. There exist a number of options for treating these effluents, such as coagulation, adsorption on activated carbon, chemical oxidation, and biological treatment. The category of Advanced Oxidation Processes (AOPs) has been identified as offering techniques with potential application for the removal of color. Many of these processes operate through the generation of free radicals ($^{\bullet}OH$), a strong oxidant species that can attack most of the organic structures found in wastewater [2,3].

Among candidate AOPs, heterogeneous photocatalysis, using particulate titanium dioxide (TiO_2) suspended in solution, has been found to eliminate color efficiently, but it requires an additional operation to remove the TiO_2 from the water [4]. Other Advanced Oxidation Processes, particularly the Fenton process [5] and the Photo-Fenton process [6], have also been shown to be effective.

The Fenton process uses iron ions as a homogeneous catalyst in the application of hydrogen peroxide as the oxidizing reagent. The Photo-Fenton system augments the Fenton process with UV radiation, apparently increasing the yield of hydroxyl radicals from the peroxide. More recently a new AOP called the Electro-Fenton process has been demonstrated; here the

---

* Corresponding author. Tel.: +52 442 2116006; fax: +52 442 2116007.
E-mail address: lgodinez@cideteq.mx (L.A. Godínez).
URL: http://www.cideteq.mx

0143-7208/$ - see front matter © 2007 Elsevier Ltd. All rights reserved.
doi:10.1016/j.dyepig.2007.01.001

hydrogen peroxide is produced *in situ* electrochemically through the cathodic reduction of dissolved oxygen on a carbon electrode according to the following reaction:

$$O_{2(g)} + 2H^+ + 2e^- \rightarrow H_2O_2 \quad (1)$$

This method, which can also be augmented by UV radiation, has been shown to be effective in destroying dyes and other organic compounds [7–13].

In general, the Fenton processes operate through the interaction of the H_2O_2 with the iron present in solution, generating the $^{\bullet}OH$ radicals according to the following reaction [14,15]:

$$H_2O_2 + Fe^{2+} \rightarrow Fe(OH)^{2+} + {}^{\bullet}OH \quad (2)$$

Furthermore, it has been shown that the application of UV light to this system, i.e. in the Photo-Fenton processes, produces additional hydroxyl radicals through the reduction of ferric ions, which could be coupled to other parallel reactions such as the photolytic breakdown of the $Fe(OH)^{2+}$ complex:

$$Fe(OH)^{2+} + h\nu \rightarrow Fe^{2+} + {}^{\bullet}OH \quad (3)$$

Thus, the combination of the electrochemical generation of H_2O_2 with the photochemical production of hydroxyl radicals, called the Photoelectro-Fenton process, generates a greater quantity of free radicals because of the contribution of both mechanisms [13,16].

Direct Photolysis (DP) of acid solutions containing peroxide on the other hand generates $^{\bullet}OH$ radicals through the homolytic breakdown of the peroxide molecule according to [17]:

$$H_2O_2 + h\nu \rightarrow 2{}^{\bullet}OH \quad (4)$$

If the UV illumination is sufficiently intense, Reaction (4) may also occur in the electrochemical processes.

In this work we compare the effectiveness of several of these water-treatment processes by studying the removal of color and total organic carbon from solutions containing the common azo dye, Orange II (OG-II). Tests were done using a batch recycle reactor operated under three conditions of interest: Direct Photolysis (DP) with hydrogen peroxide, Electro-Fenton (EF) oxidation, and the Photoelectro-Fenton (PEF) process.

2. Experimental procedure

The experiments were performed in a two-electrode concentric annular reactor containing a graphite-cloth cathode with an area of 164 cm^2 (Carbone-Lorraine Inc.) and an anode of the same material (200 cm^2) as shown in Fig. 1 [18]. The reactor volume was 250 mL, and the total solution volume, including that held in a reservoir stirred and sparged with pure oxygen, was 400 mL. The recirculating flow rate was maintained at 100 mL/min by use of a peristaltic pump (Cole Parmer Model 7553-70). In the case of photo-assisted experiments, the illumination was provided by a low-pressure UV mercury lamp (UVP Inc., $P = 75$ mW/cm^2, $\lambda = 365$ nm).

Some preliminary electrolyses were made to test the capacity of the cell to produce H_2O_2 by the cathodic reduction of dissolved oxygen in a 0.05 M solution of Na_2SO_4 adjusted to pH 3 with H_2SO_4 and saturated with oxygen. The concentration of H_2O_2 accumulated during the electrolysis was determined by titration with titanium(IV) oxysulfate [$Ti(SO_4)_2$] [19]. The experiments were performed under galvanostatic conditions.

Test solutions of dye were prepared by adding a concentration of 50 ppm of Orange II ($C_{16}H_{11}N_2NaO_4S$) to the acidified sodium sulfate solution, and the removal of color was evaluated by determining the absorbance of the solution at $\lambda = 487$ nm in a UV–vis spectrophotometer with autosampling (Agilent Technologies). Prior to the Fenton-reagent oxidation tests, ferrous sulfate solution was also added to make the ferrous concentration either 0.2 mM or 0.5 mM. For the Direct Photolysis tests, the solution contained initially 50 ppm H_2O_2, and no iron was added.

Total organic carbon (TOC) in the solutions was measured with a TOC-VSCN analyzer (Shimadzu Co), and the pH was determined with a glass-electrode pH meter (Corning 320). The Orange II dye and the titanium(IV) oxysulfate were obtained from Aldrich. Sodium sulfate, iron sulfate and sulfuric acid were obtained from J.T. Baker. Oxygen gas (Infra Co) was of reagent grade (99.99% purity), and the solutions were prepared with water type I according to the norm ASTM-D1193-$99^{\varepsilon 1}$.

3. Results and discussion

3.1. H_2O_2 accumulation in the system

The capacity of the system to generate H_2O_2 electrochemically by means of the reduction of O_2 (Reaction (1)) on the carbon-cloth cathode was studied by sampling the solution and determining the concentration of the accumulated H_2O_2 by spectrophotometric analysis. Fig. 2 shows the concentration of H_2O_2 electrochemically generated as a function of time at two different levels of applied current. Curve a corresponds to the assay in which we applied a cathodic current density $i = -100$ mA/cm^2, and Curve b was obtained with $i = -300$ mA/cm^2. In both cases it is observed that the peroxide level increases during the first 100 min of electrolysis and then levels off at constant values of 20 ppm and 50 ppm, respectively. This behavior can be explained by considering that in the steady state the rate of production of H_2O_2 is simultaneously balanced by its rate of decomposition, both at the anode and perhaps homogeneously [11,20]. From estimates of the initial slopes in Fig. 2 it appears that the net current efficiency for peroxide production is about 10% when its level in solution is negligible, and it falls off from there. On the other hand, the initial rate of accumulation and the final steady-state level of peroxide concentration for the -300 mA/cm^2 current density are about three times those for -100 mA/cm^2. Thus, there is no apparent disadvantage in operating at the higher level of current, and so subsequent oxidation tests were done at 300 mA/cm^2.

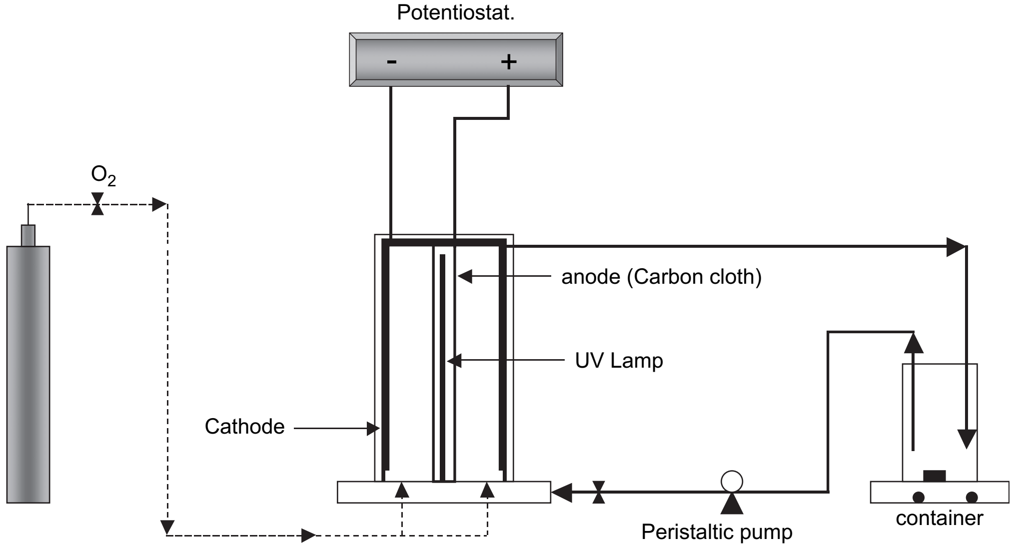

Fig. 1. Schematic diagram of the experimental reactor system.

3.2. Destruction of OG-II by the Direct Photolysis (DP) process

Fig. 3 shows the molecular structure of the model compound OG-II, which has a molecular weight of 350 g/g mol. This compound is seen to possess an azo bond (−N═N−), a benzene ring, and a naphthalene ring, which present absorbance signals at different wavelengths; the azo-bond chromophore absorbs in the visible region, while the benzene ring and the naphthalene group absorb in the UV. The UV−vis spectrum of the OG-II before oxidation is shown in Fig. 4, in which the characteristic absorbance bands are seen to fall at 228 nm, 250 nm, and 310 nm in the UV, and at 487 nm. The low-energy absorption band is assigned to the n−π* transition of the (−N═N−) group; the band at 310 nm corresponds to the π−π* transitions of the aromatic rings together with that of the (−N═N−) group of the azo dye [21].

The oxidation of the OG-II by direct photolysis (DP) using UV radiation at $\lambda = 365$ nm and 75 mW/cm^2 was tracked during the treatment time by observing the decrease in the solution absorbance at $\lambda = 487$ nm, the signal that corresponds to the maximum absorbance of this azo dye in the visible region. Samples were also analyzed for the level of TOC as a function of exposure time. The results for the decrease in solution color and the reduction of TOC using DP are shown in Fig. 5. The absorbance spectra (Fig. 5A) indicate that, although the Direct Photolysis of the hydrogen peroxide may generate the $^{\bullet}$OH species, it does not oxidize the dye very rapidly; it takes 25 min of exposure for the orange peak to be extinguished. With respect to the removal of the organic load (Fig. 5B), it is seen that TOC drops about 20% in the first 10 min of treatment, corresponding to the rapid decrease in color in this period. Subsequent to the first 10 min, there is little additional removal of TOC. After 1 h of treatment, only about 30% of TOC is removed even though the initial dose of peroxide corresponds to a 10:1 molar ratio of oxidant to dye. From these results we can infer that the degree of mineralization of the OG-II molecule to carbon dioxide and water by DP is not satisfactory.

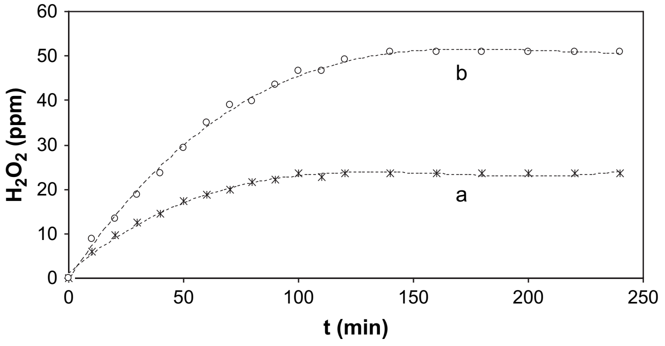

Fig. 2. Accumulation of H_2O_2 in pH 3, 0.05 M Na_2SO_4 solution in the recycle-batch electrochemical reactor of Fig. 1 at two levels of applied cathodic current density: (a) $i_c = -100$ mA/cm^2; (b) $i_c = -300$ mA/cm^2; $Q = 100$ mL/min, $V = 400$ mL.

3.3. Destruction of OG-II by the Electro-Fenton (EF) process

The next set of tests involved the continuous electrochemical generation of hydrogen peroxide in the presence of ferrous

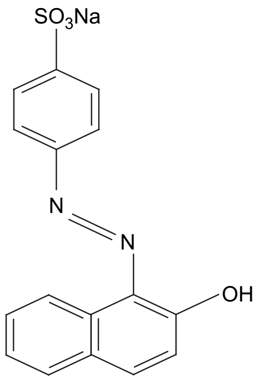

Fig. 3. Chemical structure of the Orange II azo dye.

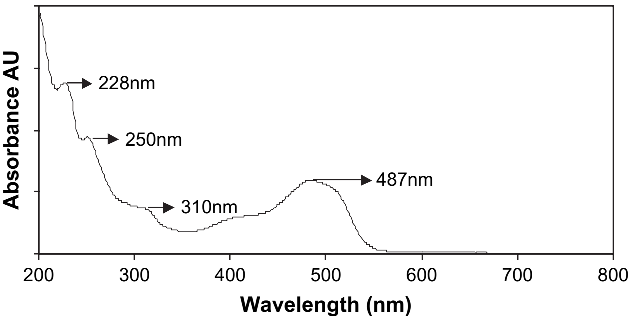

Fig. 4. UV–vis absorption spectra of Orange II azo dye solution (50 ppm) before oxidation.

ions, i.e. the Electro-Fenton (EF) process. Oxidation experiments were made at a cathode current density of −300 mA/cm^2 and at two levels of ferrous sulfate, 0.2 mM and 0.5 mM. The results are shown in Fig. 6. Fig. 6A shows the absorbance spectra of the solution from the test carried out with a concentration of 0.2 mM of the Fe^{2+}, taken at several times during the treatment, and Fig. 6B shows the corresponding results for 0.5 mM Fe^{2+}. It is seen that in both cases the orange peak in the visible region disappears almost completely within the first 5 min of treatment. It thus appears that the EF process is effective in removing color of OG-II in this system. It is interesting to note, however, that the disappearance of the visible absorbance as well as that in the UV region are both somewhat less rapid with the higher level of Fe^{2+} added to the solution.

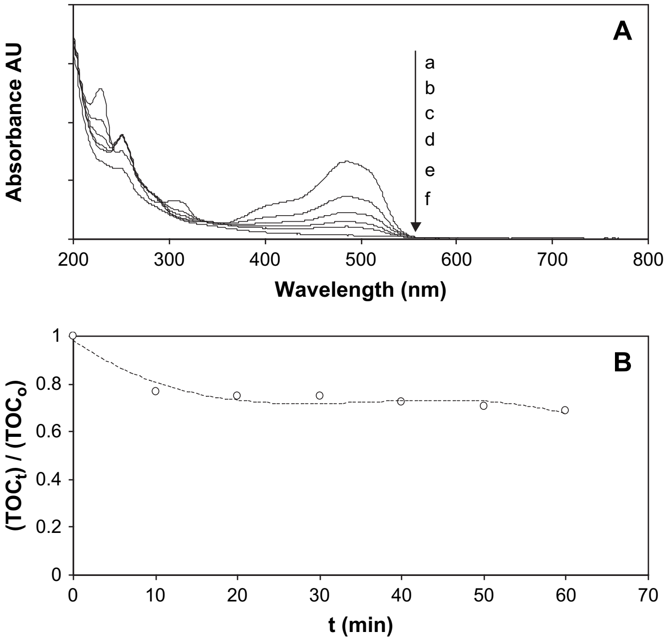

Fig. 5. (A) UV–vis absorption spectra of Orange II azo dye solution (50 ppm) treated by Direct Photolysis with an initial H_2O_2 concentration of 50 ppm in the absence of Fe^{2+}; UV-lamp illumination at $\lambda = 365$ nm and $P = 75$ mW/cm^2 after various times: (a) 0 min, (b) 5 min, (c) 10 min, (d) 15 min, (e) 20 min and (f) 25 min. (B) corresponding TOC abatement by the Direct Photolysis process.

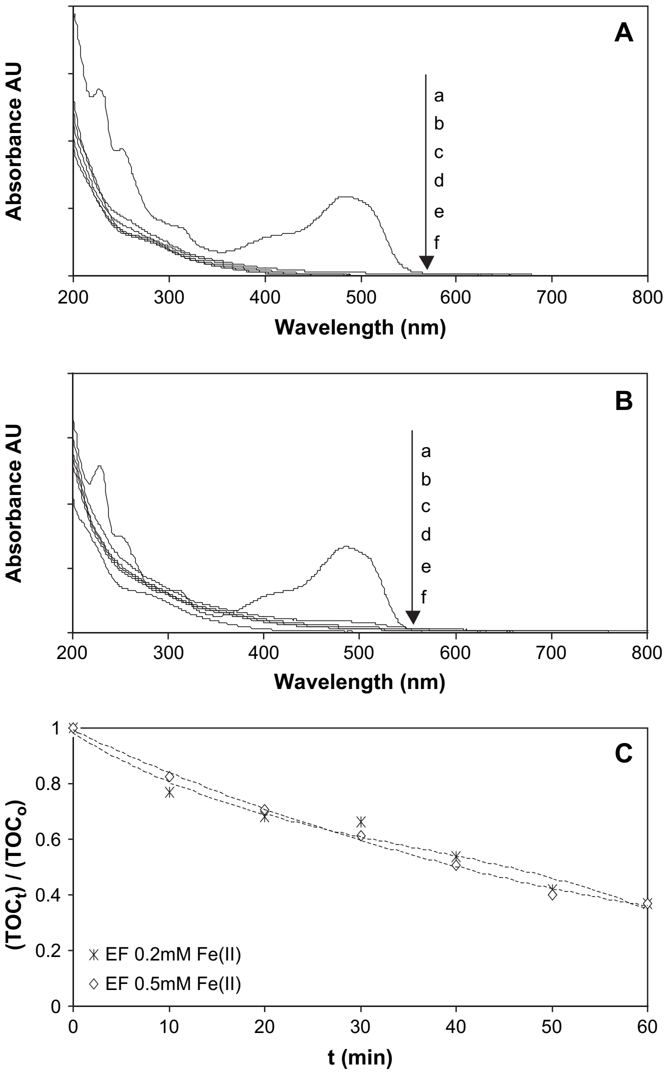

Fig. 6. UV–vis absorption spectra of Orange II azo dye solution treated with the Electro-Fenton process at various times and at two levels of ferrous ion. (A) 0.2 mM of Fe^{2+} and initially 50 ppm of H_2O_2: (a) 0 min, (b) 5 min, (c) 10 min, (d) 15 min, (e) 20 min and (f) 25 min. (B) 0.5 mM of Fe^{2+} and initially 50 ppm of H_2O_2: (a) 0 min, (b) 5 min, (c) 10 min, (d) 15 min, (e) 20 min and (f) 25 min. (C) TOC abatement in the Orange II azo dye solution by the Electro-Fenton process as a function of time with two levels of ferrous iron: (*) 0.2 mM of Fe^{2+} and initially 50 ppm of H_2O_2; (◇) 0.5 mM of Fe^{2+} and initially 50 ppm of H_2O_2.

Fig. 6C shows the reduction of TOC as a function of treatment time for the two EF tests. From this figure it appears that both levels of iron addition yield essentially the same results for TOC removal. The decrease in TOC is nearly linear with time, and the removal efficiency after 60 min is about 63%. The fact that the absorbance at 487 nm falls rapidly to near-zero levels indicates that the EF treatment attacks first the (−N=N−) bond, but the remainder of the molecule is not so readily oxidized. Thus, the level of residual TOC is significant, even after 1 h. This behavior might be explained by considering that at the beginning of the process, the iron ions react very rapidly with the H_2O_2 generating great amounts of $^{\bullet}OH$ according to Reaction (2). This active species is the one that quickly attacks the azo dye [22]. But the ions of Fe^{3+} that are generated during the EF process by Reaction (2), as well as by cathodic reduction of ferrous ions, can react with H_2O_2 to generate hydroxyperoxo radicals (${}^{\bullet}OH_2$) by the following reactions [21]:

$$Fe^{3+} + H_2O_2 \Leftrightarrow Fe{-}OOH^{2+} + H^+ \tag{5}$$

$$Fe{-}OOH^{2+} \rightarrow {}^{\bullet}OH_2 + Fe^{2+} \tag{6}$$

The ${}^{\bullet}OH_2$ radicals are less reactive than ${}^{\bullet}OH$ and thus are less effective in destroying TOC.

3.4. Removal of OG-II by the Photoelectro-Fenton (PEF) process

With the objective of increasing the OG-II destruction efficiency, we carried out a series of tests with the PEF system, a combination of the EF and DP processes. It was anticipated that introduction of UV radiation can regenerate the catalytic Fe^{2+} ion from ferric ion via Reaction (3) rather than losing oxidative power via Reactions (5) and (6). In the PEF system the generation of ${}^{\bullet}OH$ should take place according to the mechanism proposed in Eqs. (2)–(4). The same procedure was carried out as was done with the EF system, with tests done at the two different concentrations of the Fe^{2+} (0.2 mM and 0.5 mM). The results for the decrease of the absorbance signal at 487 nm for both concentrations of the Fe^{2+} are presented in Fig. 7A and 7B. The corresponding decreases in the levels of TOC are presented in Fig. 7C. The results indicate that the rate and extent of the degradation/decolorization of OG-II are much greater when the action of UV light is combined with the continuous electrochemical generation of peroxide in the presence of Fe^{2+} ions. In this case, both levels of iron ion eliminate most of the UV as well as the visible absorption within 5 min of treatment (Fig. 7A and 7B). On the other hand it is found in Fig. 7C that 0.2 mM Fe^{2+} is considerably more effective than the higher concentration, removing almost 80% of TOC within 60 min, compared to less than 50% destruction for 0.5 mM Fe^{2+}. Again, it is thought that the photo-reduction of the complex $Fe(OH)^{2+}$ to Fe^{2+} enhances the production of the ${}^{\bullet}OH$ species in the medium (via Eqs. (2) and (3)), making the oxidation process much more efficient. It is interesting to note that keeping iron levels low retards Reactions (5) and (6) and avoids depletion of the peroxide. Furthermore, higher levels of iron may also act to scavenge the active hydroxy radicals according to the following reaction [22]:

$$Fe^{2+} + {}^{\bullet}OH \rightarrow Fe^{3+} + OH^- \tag{7}$$

thus retarding the efficiency of the oxidation reactions.

3.5. Kinetics of decolorization

As was seen above, all of the treatments involving hydrogen peroxide were effective in removing the color of the Orange II dye, but some of the treatments were more rapid than the others. Presumably the disappearance of the absorption band at 487 nm results from breaking the azo bond in the dye molecule by peroxide or its derivatives. It is interesting to compare the kinetics of the various oxidation processes studied.

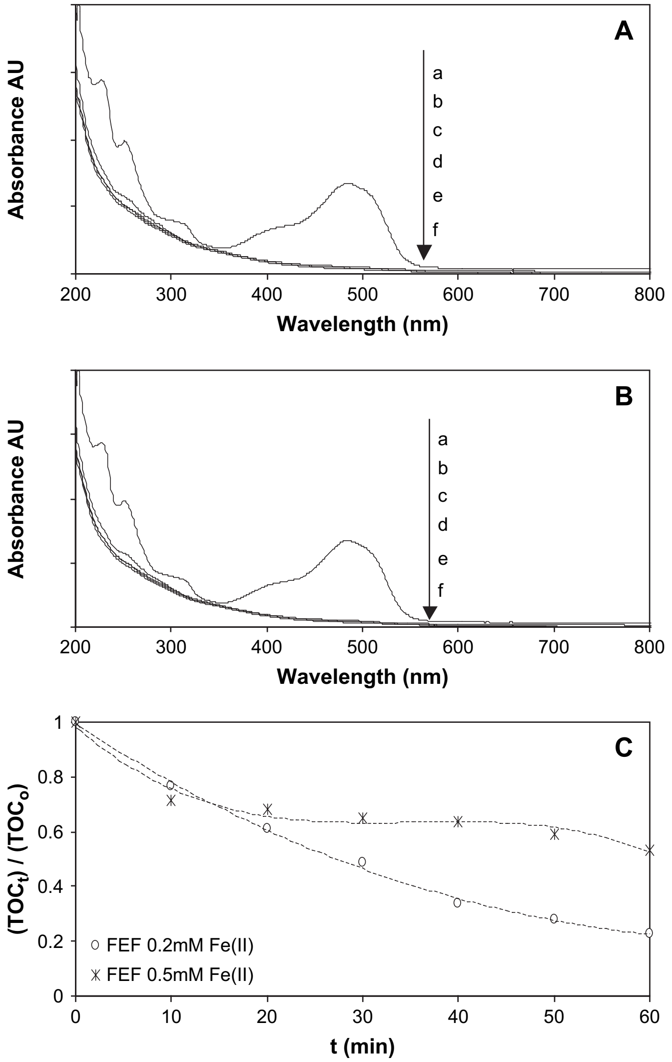

Fig. 7. UV–vis absorption spectra of the Orange II azo dye solution treated by the Photoelectro-Fenton process with UV-lamp illumination at $\lambda = 365$ nm and $P = 75$ mW/cm^2 as a function of time and at two levels of initial ferrous ion concentration. (A) 0.2 mM of Fe^{2+} and initially 50 ppm of H_2O_2: (a) 0 min, (b) 5 min, (c) 10 min, (d) 15 min, (e) 20 min and (f) 25 min; (B) 0.5 mM of Fe^{2+} and 50 ppm of H_2O_2 initially: (a) 0 min, (b) 5 min, (c) 10 min, (d) 15 min, (e) 20 min and (f) 25 min. (C) The corresponding degrees of TOC abatement: (○) 0.2 mM of Fe^{2+} and 50 ppm of H_2O_2 initially; (*) 0.5 mM of Fe^{2+} and 50 ppm of H_2O_2 initially.

In each case the initial molar concentration of the dye was 1.43×10^{-7} M, while the initial concentration of peroxide at 50 ppm was about ten times greater. Furthermore, except for the DP process, additional peroxide was produced at the anode during the treatment process. According to our interpretation of the mechanism of the oxidation processes, the main reaction in our systems is the following:

$$OG-II + {}^{\bullet}OH \rightarrow \text{oxidized products} \tag{8}$$

with the initial attack being at the azo bond. It is not possible to know the actual concentration of the active hydroxyl radical during the treatment, but a comparison of the apparent decolorization kinetics yields a practical comparison of the processes. Because of the excess of peroxide, we may assume that the overall kinetics expression for the OG-II decolorization process is pseudo-first order in the dye concentration at short times, before oxidation of the aromatic rings proceeds very far. Accordingly, the rate of disappearance of the color should follow the following first-order kinetics expression [7]:

$$\ln(C_t/C_0) = -k_1 t \tag{9}$$

where C_t is the concentration of the OG-II dye at time t, C_0 is its initial concentration, k_1 is the pseudo-first-order rate constant for decolorization, and t is time. Fig. 8 shows a plot of $\ln(C_t/C_0)$ *vs.* t for the five tests, where the concentration ratio is taken to be the observed ratio of absorbances at 487 nm. According to the linear behavior of the curves, this graph confirms the pseudo-first order of the overall decolorization kinetics. Table 1 gives the values of k_1 obtained from the slopes of these curves. It is seen that the rate constant for the Photoelectron-Fenton (PEF) process with 0.2 mM Fe^{2+} is the greatest and is more than twice as large as that for simple photolysis. The differences in the values of the rate constants presumably reflect the relative levels of available $^{\bullet}OH$ provided by each of the treatment processes.

Table 1
Values of the pseudo-first-order rate constant k_1 for the decolorization of Orange II azo dye by the various treatment processes studied

Processes	k_1 (min^{-1})
DP	0.1226
EF 0.2 mM Fe(II)	0.2364
EF 0.5 mM Fe(II)	0.2218
PEF 0.2 mM Fe(II)	0.2909
EF 0.5 mM Fe(II)	0.2097

4. Conclusions and recommendations

According to the tests carried out in this study on the treatment of weakly acidic water containing OG-II, we have seen that the decolorization and partial degradation of the dye can be achieved by any of the several peroxide-based Advanced Oxidation Processes. Furthermore, *in situ* electrochemical production of the peroxide enhances the efficiency of the processes. The addition of Fe^{2+} to the system also promotes the oxidation of the OG-II, achieving a complete decolorization of the solution in all the systems in a short time. The best performance was observed with the PEF with 0.2 mM Fe^{2+}, which can also remove 80% of the TOC within 1 h of treatment, significantly better than DF or EF that reduce the TOC by only 31% and 63%, respectively. The concentration of the iron in the system influences the performance to a considerable extent, since an excess of this catalyst becomes detrimental, probably by scavenging the active $^{\bullet}OH$ oxidant.

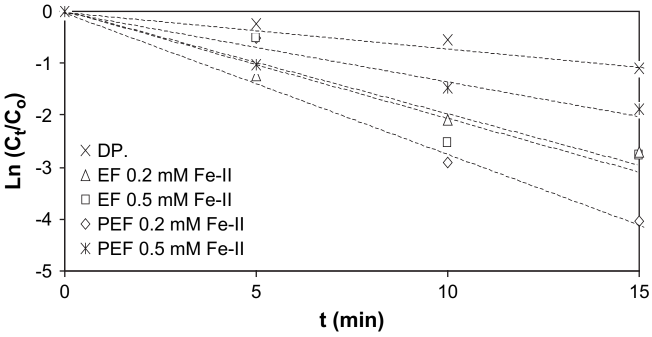

Fig. 8. First-order rate plot of azo-bond concentration, based on the optical absorption at 487 nm, showing that the decolorization reaction follows pseudo-first-order kinetics.

It is recommended that further studies be conducted on the PEF system, exploring the effects of pH, iron level, cathodic current, and reactor configuration, as well as other important target species, to optimize the efficiency and economics of its application as a wastewater-treatment process for effluents containing organic dyes.

Acknowledgments

Authors thank the Mexican Council for Science and Technology (CONACyT) and the Council for Science and Technology of Guanajuato (CONCyTEG) for financial support of this work (Grant GTO-04-C02-68). J.M.P.H. also acknowledges CONACyT for a graduate fellowship, Prof. Sixto Malato at PSA (Spain) for a scholar internship and Prof. José Luis Jurado for his invaluable comments and suggestions.

References

[1] Augugliaro V, Baiocchi C, Bianco Prevot A, García-López E, Loddo V, Malato S, et al. Azo-dyes photocatalytic degradation in aqueous suspension of TiO_2 under solar irradiation. Chemosphere 2002;49:1223–30.
[2] Andreozzy R, Caprio V, Insola A, Marotta R. Advanced oxidation processes (AOP) for water purification and recovery. Catal Today 1999;53:51–9.
[3] Gogate Parag R, Pandit Aniruddha B. A review of imperative technologies for wastewater treatment I: oxidation technologies at ambient conditions. Adv Environ Res 2004;8:501–51.
[4] Bauer Ch, Jacques P, Kalt A. Photooxidation of azo dye induced by visible light incident on the surface of TiO_2. J Photochem Photobiol A 2001;140:87–92.
[5] Solozhenko EG, Soboleva NM, Goncharuk VV. Decolourization of azo dye solutions by Fenton's oxidation. Water Res 1995;29:2206–10.
[6] Pérez M, Torrades F, Doménech X, Peral J. Fenton and photo-Fenton oxidation of textile effluents. Water Res 2002;36:2703–10.
[7] Oturan Mehmet A, Oturan Nihal, Lahitte C, Trevin S. Production of hydroxyl radicals by electrochemically assisted Fenton's reagent. Application to the mineralization of an organic micropollutant pentachlorophenol. J Electroanal Chem 2001;507:96–102.
[8] Aaron Jean J, Oturan Mehmet A. New photochemical and electrochemical methods for the degradation of pesticides in aqueous media. Environmental applications. Turk J Chem 2001;25:509–20.
[9] Gözmen B, Oturan Mehmet A, Oturan N, Erbatur O. Indirect electrochemical treatment of bisphenol A in water via electrochemically generated Fenton's reagent. Environ Sci Technol 2003;37:3716–23.
[10] Alvarez-Gallegos A, Pletcher D. The removal of low-level organics via hydrogen peroxide formed in a reticulated vitreous carbon cathode

cell. Part 1: the electrosynthesis of hydrogen peroxide in aqueous acidic solutions. Electrochim Acta 1998;44:852–61.

[11] Wang A, Qu J, Ru J, Liu H, Ge J. Mineralization of an azo dye Acid Red 14 by electro-Fenton's reagent using an activated carbon fiber cathode. Dyes Pigments 2005;65:227–33.

[12] Da Pozzo A, Di Palma L, Merli C, Petricci E. An experimental comparison of a graphite electrode and a gas diffusion electrode for the cathodic production of hydrogen peroxide. J Appl Electrochem 2005;35:413–9.

[13] Brillas E, Baños MA, Camps S, Arias C, Cabot Pere-Lluís, Garrido JA, et al. Catalytic effect of Fe^{2+}, Cu^{2+} and UVA light on the electrochemical degradation of nitrobenzene using an oxygen-diffusion cathode. New J Chem 2004;28:314–22.

[14] Brillas E, Mur E, Sauleda R, Sánchez L, Peral J, Doménech X, et al. Aniline mineralization by AOP's: anodic oxidation, photocatalysis, electro-Fenton and photoelectro-Fenton processes. Appl Catal B Environ 1998; 16:31–42.

[15] Brillas E, Baños MA, Garrido JA. Mineralization of herbicide 3,6-dichloro-2-methoxybenzoic acid in aqueous medium by anodic oxidation, electro-Fenton and photoelectron-Fenton. Electrochim Acta 2003;48: 1697–705.

[16] Boye B, Dieng Momar M, Brillas E. Degradation of herbicide 4-chlorophenoxyacetic acid by advanced electrochemical oxidation methods. Environ Sci Technol 2002;36:3030–5.

[17] Rathi A, Rajor Hament K, Sharma Rakesh K. Photodegradation of Direct Yellow-12 using $UV/H_2O_2/Fe^{2+}$. J Hazard Mater B 2003;102: 231–41.

[18] Peralta-Hernández JM, Meas-Vong Y, Rodriguez Francisco J, Chapman Thomas W, Maldonado Manuel I, Godínez Luis A. *In situ* electrochemical and photo-electrochemical generation of the Fenton reagent: a potentially important new water treatment technology. Water Res 2006;40:1754–62.

[19] Eisenberg George M. Colorimetric determination of hydrogen peroxide. Ind Eng Chem 1943;15:327–8.

[20] Chen J, Liu M, Zhang L, Zhang J, Jin L. Application of nanoTiO_2 towards polluted water treatment combined with electro-photochemical method. Water Res 2003;37:3815–20.

[21] Ramirez J Herney, Costa A Carlos, Madeira M Luis. Experimental design to optimize the degradation of the synthetic dye Orange II using Fenton's reagent. Catal Today 2005;107:68–76.

[22] Malik PK, Saha SK. Oxidation of direct dyes with hydrogen peroxide using ferrous ions as catalyst. Sep Purif Technol 2003;31:241–50.